

Two-Impurity Kondo Effect in Double-Quantum-Dot Systems — Effect of Interdot Kinetic Exchange Coupling —

Wataru Izumida*

Department of Applied Physics, Hokkaido University, Sapporo 060-8628, Japan

Osamu Sakai

Department of Physics, Tokyo Metropolitan University, Tokyo 192-0397, Japan

Tunneling conductance through two quantum dots, which are connected in series to left and right leads, is calculated by using the numerical renormalization group method. As the hopping between the dots increases from very small value, the following states continuously appear; (i) Kondo singlet state of each dot with its adjacent-site lead, (ii) singlet state between the local spins on the dots, and (iii) double occupancy in the bonding orbital of the two dots. The conductance shows peaks at the transition regions between these states. Especially, the peak at the boundary between (i) and (ii) has the unitarity limit value of $2e^2/h$ because of coherent connection through the lead-dot-dot-lead. For the strongly correlated cases, the characteristic energy scale of the coherent peak shows anomalous decrease relating to the quantum critical transition known for the two-impurity Kondo effect. The two dots systems give the new realization of the two-impurity Kondo problem.

PACS 73.40.Gk, 72.15.Qm, 73.23.Hk

I. INTRODUCTION

Dilute magnetic impurities in metal bring the single-impurity Kondo effect [1,2]. The anti-ferromagnetic coupling between spins on impurities J , such as the RKKY interaction, would compete with the Kondo effect. To study such competition effect, the two impurities in metal have been studied extensively [3–14]. If the Kondo binding energy is much larger than J ($T_K \gg J$), each local spin on the magnetic impurity forms the Kondo singlet state with the conduction electrons. On the other hand for $T_K \ll J$, the two local spins form the local spin singlet state. From the numerical renormalization group (NRG) calculation, Jones *et al.* had pointed out that the transition between the two states occurs as a quantum critical phenomenon [4]. However the advanced investigation made clear that the critical transition is an artifact of the model neglecting the parity splitting terms, such as the d-d hopping term between the impurity atoms [8]. In this paper we will investigate the effect of the d-d hopping term in double-quantum-dot (DQD) systems in detail, and give the new realization to the two-impurity Kondo problem.

It might be difficult to observe the two-impurity effect in metal systems as pointed out by previous studies, because the alloy contains many types of impurity pairs, and because the coupling between impurities is fixed in each material. Recently, the Kondo effect is observed in the single quantum dot systems [15–19]. The experimental data show good agreement with the results of numerical calculation based on the single-impurity Anderson model [20]. These works demonstrated that the quantum dot systems are suitable for sensitive experiment of the Kondo problem. On the DQD systems, each dot corresponds to an impurity atom, and the coupling between

the dots can be changed freely by applying the split gate voltage between the dots [21]. It would be expected that we can investigate the two-impurity effect systematically in the DQD systems.

For the DQD systems, which the two dots are connected to the left lead and the right lead in series as ‘lead-dot-dot-lead’, there are several theoretical works including the Kondo effect [22–27]. We have reported the large enhancement of the tunneling conductance through the two dots when the condition $J_{LR}^{\text{eff}} \sim T_K^0$ holds, by using the NRG calculation [25]. Here $J_{LR}^{\text{eff}} = 4t^2/U$ is the anti-ferromagnetic kinetic exchange coupling between the two dots, t is the hopping between the two dots, U is the Coulomb repulsion on the dot, and T_K^0 is the Kondo temperature at $t = 0$. We note that the anti-ferromagnetic coupling is the inevitable effect due to the kinetic process t and the Coulomb repulsion on the dot U . There are investigations with the slave boson mean field theory (SBMFT). Aono *et al.* had already studied the same model of us, however they could not find the relation $J_{LR}^{\text{eff}} \sim T_K^0$ on the peak of the conductance pointed out by us because the SBMFT can not treat the kinetic exchange process properly [24]. Georges *et al.* introduced the anti-ferromagnetic coupling J between the two dots by artifact in the model, and discussed the effect related to the critical transition on the conductance by using the SBMFT [26]. However the introduction of the artificial J in the model and the calculation of the conductance within the SBMFT framework bring some questions as follows: (a) Does the effect of anti-ferromagnetic coupling pointed by Georges *et al.* actually appear in the DQD systems?, because the hopping itself breaks the quantum critical transition [8,9]. If it appears, however, (b) how the conflicting effects of t , the kinetic exchange coupling that would cause the critical transition and the parity splitting that suppress the critical transition, compete?

And then, (c) how they appear in the conductance? Since the SBMFT could not treat the kinetic exchange process properly, this approximation for the two-impurity Kondo problem like the DQD systems seems to be unfavorable. The reliable calculation is necessary for such a sensitive problem.

In this paper, we present the detailed investigation of the Kondo effect in the DQD systems. The numerical calculation is performed by using the NRG method. This numerical method is known to be a reliable one for the two-impurity Kondo problem [3–6,8,9,14]. We calculate the tunneling conductance through the two dots. We note that some preliminary results were presented at SCES98 [25], and the one of the central results was presented at LT22 [27].

We find that the following states continuously appear when the hopping between the two dots increases from very small value; (i) Kondo singlet state ($t \ll U$, $J_{\text{LR}}^{\text{eff}} \ll T_{\text{K}}^0$), (ii) singlet state between local spins on the dots ($t \ll U$, $J_{\text{LR}}^{\text{eff}} \gg T_{\text{K}}^0$), and (iii) double occupancy in the bonding orbital of the two dots ($t \gtrsim U$). The conductance shows peaks at the transition regions between these states. The ‘main peak’ at the boundary between (i) and (ii) with the condition $J_{\text{LR}}^{\text{eff}} \sim T_{\text{K}}^0$ has the unitarity limit value of $2e^2/h$ because of coherent connection through the lead-dot-dot-lead. Especially for the strongly correlated cases, the width of the main peak becomes very narrow and the characteristic temperature of the peak is largely suppressed compared with the Kondo temperature of the single dot systems T_{K}^0 . These anomalies of the main peak closely relate to the quantum critical phenomenon in the two-impurity Kondo problem. The quantitative calculation in this paper gives the new realization for the two-impurity Kondo problem, and suggests the possibility of the systematic study of the anomalous two-impurity Kondo effect in the DQD systems.

The formulation is presented in §II. The numerical results are presented in §III. The summary and discussion are given in §IV.

II. FORMULATION

We investigate the following model Hamiltonian for the DQD systems that the two dots are connected to the left lead and the right lead in series;

$$H = H_1 + H_d + H_{1-d}, \quad (1)$$

$$H_1 = \sum_{k\sigma} \varepsilon_k c_{Lk\sigma}^\dagger c_{Lk\sigma} + \sum_{q\sigma} \varepsilon_q c_{Rq\sigma}^\dagger c_{Rq\sigma}, \quad (2)$$

$$\begin{aligned} H_d &= \varepsilon_{d,L} \sum_{\sigma} n_{d,L\sigma} + \varepsilon_{d,R} \sum_{\sigma} n_{d,R\sigma} \\ &+ (-t \sum_{\sigma} d_{L\sigma}^\dagger d_{R\sigma} + \text{h.c.}) \\ &+ U_L n_{d,L\uparrow} n_{d,L\downarrow} + U_R n_{d,R\uparrow} n_{d,R\downarrow}, \end{aligned} \quad (3)$$

$$H_{1-d} = \sum_{k\sigma} V_{Lk} d_{L\sigma}^\dagger c_{Lk\sigma} + \sum_{q\sigma} V_{Rq} d_{R\sigma}^\dagger c_{Rq\sigma} + \text{h.c.} \quad (4)$$

H_1 gives the electrons in the left and right leads. H_d gives that in the left and right dots. H_{1-d} gives the tunneling between the left lead and the left dot, and between the right lead and the right dot. The suffices L, R mean the left and the right, respectively. $c_{Lk\sigma}$ is the annihilation operator of the electron in the left lead, $d_{L\sigma}$ is that in the left dot. $n_{d,L\sigma} = d_{L\sigma}^\dagger d_{L\sigma}$ is the number operator of the left dot. ε_k is the energy of the state k in the left lead. $\varepsilon_{d,L}$ is the energy of the orbital in the left dot. The quantity t is the matrix element between the left and right dots, and we call it as the ‘hopping’ between the dots hereafter. U_L is the Coulomb interaction between the electrons in the left dot. V_L is the matrix element between the left dot and the left lead.

Here we consider only the single orbital in each of the dots. This situation is justified in the case that the typical energy splitting between the orbitals in the dot is larger than the typical broadening of the energy levels, $\delta\varepsilon_d \gg \Delta$, and when the temperature is smaller than the typical Coulomb repulsion between the electrons in the dots, $T \ll U$ [20,28]. (The Kondo effect is not important in the case of $T \gtrsim U$.) We consider only the on-site Coulomb interaction between the electrons. Furthermore, we consider only the nearest neighboring tunneling, between the dot and its adjacent-site lead, between the two dots. The energies $\varepsilon_{d,L}$, $\varepsilon_{d,R}$ can be changed by applying the gate voltage on the dots. V_{Lk} (V_{Rq}) can also be changed by applying the split gate voltage between the left (right) dot and the left (right) lead. t can be changed by applying the split gate voltage between the left dot and the right dot.

In this paper we consider only the symmetric case with respect to the exchange of the left and the right. This situation is written with the following relations; $\varepsilon_d \equiv \varepsilon_{d,L} = \varepsilon_{d,R}$, $U \equiv U_L = U_R$, and $\Delta \equiv \Delta_L = \Delta_R = \pi|V|^2\rho_c$. (Δ is the hybridization strength between the dots and the leads, $V \equiv V_{Lk} = V_{Rk}$, ρ_c is the density of states in the leads. Here we consider that there are no k -dependence in the matrix element and the density of states.) The model can be mapped into the two-channel Anderson Hamiltonian by the unitary transform for the operators of the dots and the operators of the leads [25]. Furthermore we consider the situation that there is one electron in each dot by adjusting the gate voltage on the dot, $\langle n_{d,L} \rangle = 1$, $\langle n_{d,R} \rangle = 1$.

We solve the Hamiltonian by using the NRG method, and calculate the conductance from the current correlation function within the linear response theory [25,28,29]. (For detailed calculation of the conductance, see appendix of Ref. [29].)

At zero temperature, the conductance can be rewritten by using the effective parameters of the fixed point non-interacting Anderson Hamiltonian as follows;

$$G = \frac{2e^2}{h} |\Delta\mathcal{G}_e(0^+) - \Delta\mathcal{G}_o(0^+)|^2$$

$$= \frac{2e^2}{h} \frac{4(t^{\text{eff}}/\Delta^{\text{eff}})^2}{(1 + (t^{\text{eff}}/\Delta^{\text{eff}})^2)^2}. \quad (5)$$

We have used the relation, $\mathcal{G}_p = z_p/(\omega - \varepsilon_p^{\text{eff}} + i\Delta_p^{\text{eff}})$, $z_p = \Delta_p^{\text{eff}}/\Delta$, ($p = e, o$) at $T = 0$. Here the suffix p denote the even and odd parity orbitals in the two dots. We note that the even orbital is the bonding orbital, and the odd orbital is the anti-bonding orbital. We now consider the case of $\langle n_e \rangle + \langle n_o \rangle = 2$, then $t^{\text{eff}} \equiv -\varepsilon_e^{\text{eff}} = \varepsilon_o^{\text{eff}} \geq 0$, $\Delta^{\text{eff}} \equiv \Delta_e^{\text{eff}} = \Delta_o^{\text{eff}}$. Here t^{eff} is the effective hopping between the dots, and Δ^{eff} is the effective hybridization strength between the leads and the dots. At $T = 0$, we calculate the effective parameters from the analysis of the flow chart of the renormalized energy level structure in the NRG calculation, and then calculate the conductance from eq. (5).

III. NUMERICAL RESULTS

In numerical calculation we choose the half of the band width as an energy unit. The Coulomb repulsion is fixed at $U = 0.1$ through this paper. We calculate the conductance as a function of the hopping t for various hybridization strength Δ . (As noted in previously, t and Δ can be changed by applying the split gate voltage between the dots, between the dots and the leads, respectively.) The gate voltage on the dots is fixed at $\varepsilon_d = -U/2$, then the DQD is in the half-filled case, i. e. each dot contains one electron.

In §III A and §III B we present the numerical results at zero temperature $T = 0$, and in §III C we present the results at finite temperatures.

A. Conductance in the strongly correlated case

First we present the conductance in the strongly correlated case with the hybridization strength satisfying $\Delta/\pi = 1.5 \times 10^{-3}$, ($\Delta/\pi U = 1.5 \times 10^{-2}$, i.e. $u \equiv U/\pi\Delta \simeq 6.8$).

We show the conductance at $T = 0$ as a function of the hopping t in Fig. 1. (The occupation number and the phase shift are also shown in Fig. 1.) There are two peaks in the conductance, the large peak near $t \sim 5 \times 10^{-4}$, and the small peak near $t \sim 2 \times 10^{-2}$. (Hereafter we call the large peak as the ‘main peak’.) Why these peaks appear? In the later paragraph we will analyze various quantities for the parameter cases showing the peaks.

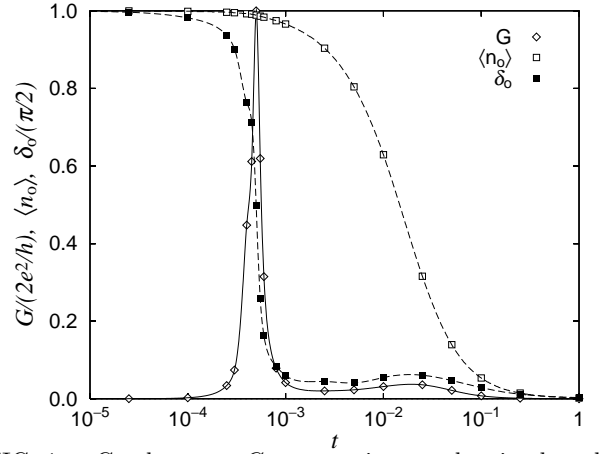


FIG. 1. Conductance G , occupation number in the odd orbital of the two dots $\langle n_o \rangle$, and phase shift of the odd channel δ_o , as a function of the hopping t at $T = 0$. We note the relations between the even and odd orbitals, $\langle n_e \rangle = 2 - \langle n_o \rangle$, $\delta_e = \pi - \delta_o$. $\Delta/\pi U = 1.5 \times 10^{-2}$.

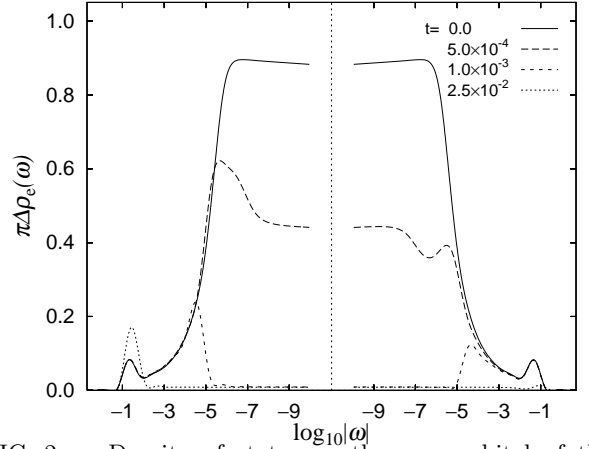


FIG. 2. Density of states on the even orbital of the two dots, $\rho_e(\omega)$. We note the relation $\rho_o(\omega) = \rho_e(-\omega)$, where $\rho_o(\omega)$ is the density of states on the odd orbital. $\Delta/\pi U = 1.5 \times 10^{-2}$.

The density of states on the even orbital of the two dots, $\rho_e(\omega)$, for several t cases is shown in Fig. 2. (The relation $\rho_e(\omega) = \rho_o(-\omega)$ holds for $\langle n_e \rangle + \langle n_o \rangle = 2$, where $\rho_o(\omega)$ is the density of states on the odd orbital of the two dots.) At $t = 0$, there is the Kondo peak on the Fermi energy. (Fermi energy corresponds to $\omega = 0$.) Naturally, this Kondo peak is caused by the Kondo singlet states between the left lead and the left dot, and between the right lead and the right dot. As t increases to $t = 5 \times 10^{-4}$, the conductance has the main peak and the strength of $\rho_e(\omega \sim 0)$ becomes half of that at $t = 0$. In this region we can consider that the Kondo effect with the spins on the orbitals extending the two dots, the even and the odd orbitals, occurs. As t still increases, the conductance decreases rapidly, and the strength of $\rho_e(\omega \sim 0)$ is largely suppressed as shown at $t = 1.0 \times 10^{-3}$. This suppression means the disappearance of the Kondo coupling

between the leads and the dots. t becomes still large, the conductance has the small peak at $t \sim 2 \times 10^{-2}$. At $t = 2.5 \times 10^{-2}$, the density of states on the even and odd orbitals have peaks at $\mp\omega \sim 10^{-1}$, respectively, from Fig. 2. At the same time the occupation numbers begin to change as shown in Fig. 1. ($\langle n_e \rangle \simeq 1.5$, $\langle n_o \rangle \simeq 0.5$ at $t \simeq 1.5 \times 10^{-2}$.)

Here we note the following two points: First, the condition $J_{\text{LR}}^{\text{eff}} \sim T_{\text{K}}^0$ holds at $t \simeq 5 \times 10^{-4}$, where $J_{\text{LR}}^{\text{eff}} \equiv 4t^2/U$. ($T_{\text{K}}^0 = 3.78 \times 10^{-6}$ is the Kondo temperature at $t = 0$, with the expression $T_{\text{K}}^0 = \sqrt{U\Delta/2} \exp[-\pi U/8\Delta + \Delta/2U]$ [1], then $J_{\text{LR}}^{\text{eff}}/T_{\text{K}}^0 \simeq 2.65$ at $t = 5.0 \times 10^{-4}$.) Second, as seen from Fig. 1, the occupation numbers of the even and the odd orbitals for $t \lesssim 1.0 \times 10^{-3}$ are almost same with each other, $\langle n_e \rangle \simeq \langle n_o \rangle \simeq 1$. For $t \gtrsim 1.0 \times 10^{-1}$, the two electrons occupy the even orbital. The border between them is at $t \sim U/4 (= 2.5 \times 10^{-2})$.

Above analysis implies the following scenario. In the case of $t \ll U/4 (= 2.5 \times 10^{-2})$, the hopping t causes the anti-ferromagnetic kinetic exchange coupling, $J_{\text{LR}}^{\text{eff}}$. For smaller hopping case with $J_{\text{LR}}^{\text{eff}} \ll T_{\text{K}}^0$, there are the Kondo singlet states between the left lead and the left dot, and between the right lead and the right dot each other. As t increases and then $J_{\text{LR}}^{\text{eff}} \gg T_{\text{K}}^0$, the two local spins on each dot form the local singlet state. At the transition region between two states we have a main peak with the unitarity limit value of $2e^2/h$ in the conductance. This will indicate that the leads and the dots are coherently connected by the even and the odd orbital states. When t becomes still large and the condition $t \gtrsim U/4$ holds, the local spins do not appear, instead, the two electrons occupy the even orbital. The small peak of the conductance reflects the transition of the electronic states in the DQD.

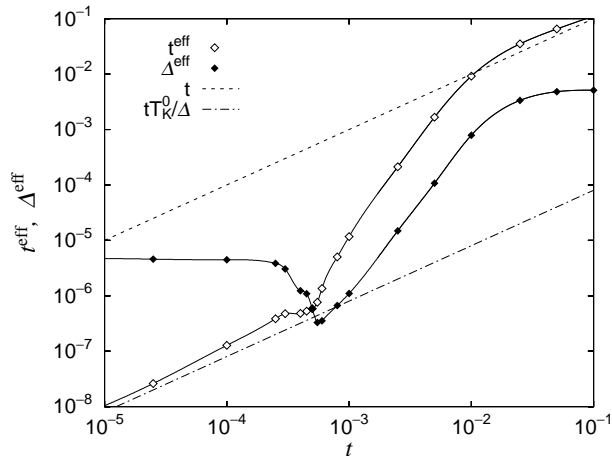


FIG. 3. Effective parameters t^{eff} , Δ^{eff} of the fixed point non-interacting Anderson Hamiltonian, given by the analysis of the flow chart of the renormalized energy level structure in the NRG calculation. $\Delta/\pi U = 1.5 \times 10^{-2}$.

Here we show the effective parameters t^{eff} and Δ^{eff} as a function of t in Fig. 3. (We note that the effective parameters have been used already for the calculation of

the conductance shown in Fig. 1.) In $t \lesssim 10^{-4}$ case, the effective parameters behave as $t^{\text{eff}} \sim tT_{\text{K}}^0/\Delta$, $\Delta^{\text{eff}} \sim T_{\text{K}}^0$. Then the conductance coincides with the non-interacting one when one substitutes the effective parameters into eq. (5). As t increases with the condition near $J_{\text{LR}}^{\text{eff}} \sim T_{\text{K}}^0$, Δ^{eff} once decreases, and it has local minimum, and then it increases. At the same time the slope of t^{eff} once decreases and then increases. When t^{eff} and Δ^{eff} coincide with each other, the conductance has a peak at $t \sim 5 \times 10^{-4}$, i. e. $J_{\text{LR}}^{\text{eff}} \sim T_{\text{K}}^0$. As t increases slightly beyond this point, the conductance sharply decreases because Δ^{eff} decreases to the minimum even though t^{eff} increases. Here we stress that the relation $J_{\text{LR}}^{\text{eff}} \sim T_{\text{K}}^0$ holds when $t^{\text{eff}} \sim \Delta^{\text{eff}}$, and at the same time Δ^{eff} becomes very small in the transition region. When t increases further, the ratio $t^{\text{eff}}/\Delta^{\text{eff}}$ increases gradually in the region $t \lesssim U/4 (= 2.5 \times 10^{-2})$. At $t \sim U/4$, the ratio $t^{\text{eff}}/\Delta^{\text{eff}}$ begins to decrease and then increases. Therefore the conductance shows a broad peak near the region $t \sim U/4$. For $t \gtrsim U/4$ case, the effective parameters behave $t^{\text{eff}} \sim t$, $\Delta^{\text{eff}} \sim \Delta$. We note that the conductance has the expression of the non-interacting one itself in $t \gtrsim U/4$ region.

Finally we compare between the phase shift and the occupation number shown in Fig. 1. The phase shift of the odd orbital δ_o rapidly changes from $\pi/2$ to 0 near $t \sim 5 \times 10^{-4}$, even though $\langle n_o \rangle$ still remains at $\langle n_o \rangle \sim 1$. Friedel's sum rule in each channel does not hold, as already pointed out previously [9]. It seems that this behavior is enhanced when the anti-ferromagnetic coupling between the two sites competes with the Kondo effect.

B. From Weakly to Strongly correlated cases

In this subsection we present the numerical results of the conductance for various $\Delta/\pi U$ cases within $1.5 \times 10^{-2} \leq \Delta/\pi U \leq 6.0 \times 10^{-2}$. ($1.7 \lesssim u \lesssim 6.8$. The hybridization strength is changed in $1.5 \times 10^{-3} \leq \Delta/\pi \leq 6.0 \times 10^{-3}$, and the Coulomb repulsion is fixed at $U = 0.1$.) We confirm the scenario shown in the previous subsection that $J_{\text{LR}}^{\text{eff}} \sim T_{\text{K}}^0$ holds at the main peak of the conductance with $t^{\text{eff}} \sim \Delta^{\text{eff}}$. We also demonstrate how the kinetic exchange process appear in the conductance for arbitrary $\Delta/\pi U$ cases.

The calculated conductance is shown in Fig. 4. The horizontal axis is the hopping normalized by the hybridization strength, t/Δ . From inset of the Fig. 4, the conductance almost overlaps on the non-interacting curve in the region $t \ll \Delta$ and $t \gg \Delta$. Exactly, these regions should be classified $J_{\text{LR}}^{\text{eff}} \ll T_{\text{K}}^0$ and $t \gg U/4$, respectively, from the analysis in the previous subsection. The conductance is very small in these regions, however this uniform properties should be useful to arrange the experimental data under uncertain U/Δ cases.

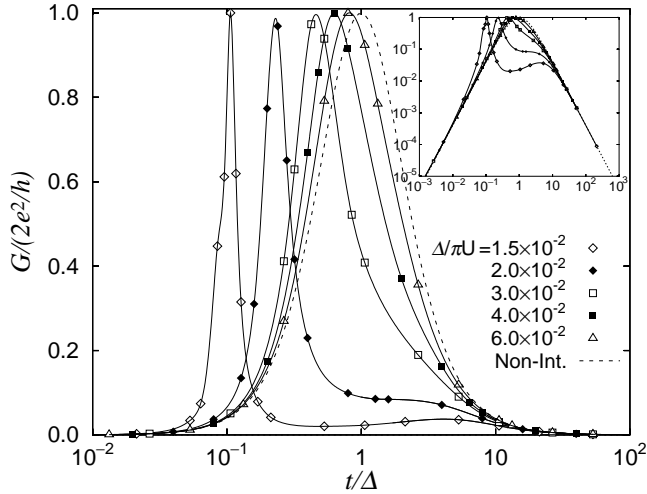


FIG. 4. Conductance as a function of t at zero temperature, from the weakly to strongly correlated cases in $1.5 \times 10^{-2} \leq \Delta/\pi U \leq 6.0 \times 10^{-2}$. The broken line shows the conductance for the non-interacting ($U=0$) case.

All curves have a main peak with strength $2e^2/h$. For weakly correlated cases of $\Delta/\pi U \gtrsim 4 \times 10^{-2}$, the conductance almost coincides with the non-interacting one through all t region. As U/Δ increases, the main peak shifts to the small t/Δ side, and the peak width becomes narrower.

We already found the relation $J_{LR}^{\text{eff}} \sim T_K^0$ at the main peak position for $\Delta/\pi U = 1.5 \times 10^{-2}$ case in §III A. Here we show the ratio $J_{LR}^{\text{eff}}/T_K^0$ at the main peak position for various $\Delta/\pi U$ cases in Table I. We can see the relation $J_{LR}^{\text{eff}} \sim T_K^0$ commonly [25]. (The relation at the main peak, $J_{LR}^{\text{eff}} \sim T_K^0$, would be generalized to $E_B \sim T_K^0$ to the weakly correlated cases, where $E_B = \sqrt{(2t)^2 + (U/2)^2} - U/2$ is the singlet binding energy between the two dots.)

From the analysis in the previous and present subsection we can conclude the following effect of the hopping term. For the small t case with $J_{LR}^{\text{eff}} \ll T_K^0$, “(i) The Kondo singlet state is formed on the left (right) dot with

its adjacent-site lead”. On the other hand for the large t case with $J_{LR}^{\text{eff}} \gg T_K^0$, “(ii) the local spins on each of the dots couple as the singlet state”. In the intermediate region, the Kondo effect of the local spins on the orbitals extending on the two dots (i.e. even and odd orbitals) occurs. The main peak of the conductance appears around the boundary between (i) and (ii) reflecting the coherent connection of the leads and the dots. As U/Δ increases, the Kondo temperature T_K^0 exponentially decreases, the condition $J_{LR}^{\text{eff}} \sim T_K^0$ holds at the smaller t/Δ , then the main peak shifts to the smaller t/Δ side. At the same time, the width of the peak becomes extremely narrow compared with the decreasing of T_K^0 . This fact has been already shown as the steep minimum of Δ^{eff} in Fig. 3. We note that this narrowing closely relates to the quantum critical transition between the Kondo singlet state and the local singlet state in the two-impurity Kondo model [4]. The shifting and narrowing behaviors shown here are also pointed out with the SBMFT with artificial addition of the anti-ferromagnetic coupling between dots to the model [26]. However, the SBMFT calculation should be checked by the method treating the kinetic exchange term properly. As noted in the introduction, the hopping term causes two conflicting effects on the critical transition of the two-impurity systems. One is the kinetic exchange coupling J_{LR}^{eff} , which causes the “critical” transition through the competition with the Kondo effect. Another is the parity splitting, which suppresses the “critical” transition. The calculation in this section is the first reliable quantitative results of the two-impurity Kondo problem in the DQD systems.

There is also another small peak (or shoulder) structure for the strongly correlated cases of $\Delta/\pi U \lesssim 2 \times 10^{-2}$ ($u \gtrsim 5$) at larger t side of the main peak. In the previous subsection, we found that the small peak appears around the boundary between (ii) and (iii). However for the weakly correlated cases, the small peak could not be recognized because the condition of the border (i)-(ii) and (ii)-(iii) could not be distinguished clearly.

$\Delta/\pi U$	1.5×10^{-2}	2×10^{-2}	3×10^{-2}	4×10^{-2}	6×10^{-2}
$J_{LR}^{\text{eff}}/T_K^0$	2.66	2.34	2.15	2.09	2.23
E_B/T_K^0	2.66	2.34	2.14	2.04	2.05

TABLE I. Ratios $J_{LR}^{\text{eff}}/T_K^0$ and E_B/T_K^0 at the main peak position of the conductance.

C. Temperature dependence of the conductance

In this subsection we present the conductance in finite temperature. We calculate the conductance at finite temperatures by using the following formula [29];

$$G = \frac{2e^2}{h} \lim_{\omega \rightarrow 0} \frac{P''(\omega)}{\omega}. \quad (6)$$

Here $P''(\omega)$ is the ‘current spectrum’ for the current operator $J \equiv \dot{N}_L - \dot{N}_R$ written as follows,

$$P''(\omega) = \frac{\pi^2 \hbar^2}{4} \frac{1}{Z} \sum_{n,m} (e^{-\beta E_m} - e^{-\beta E_n}) \times |\langle n | J | m \rangle|^2 \times \delta(\omega - (E_n - E_m)), \quad (7)$$

where \dot{N}_L is the time differentiation of the electron number in the left lead, $Z = \sum_n e^{-\beta E_n}$ is the partition function of the system, and β is the inverse of the temperature ($\beta = 1/T$).

First we show the conductance at various temperatures for $\Delta/\pi U = 1.5 \times 10^{-2}$ case in Fig. 5. As the temperature increases from $T \sim 10^{-8}$, the height of the main peak gradually decreases. At the same time the peak position shifts to the larger t . We note that $T \sim 10^{-8}$ is much lower than T_K^0 . ($T_K^0 = 3.78 \times 10^{-6}$.)

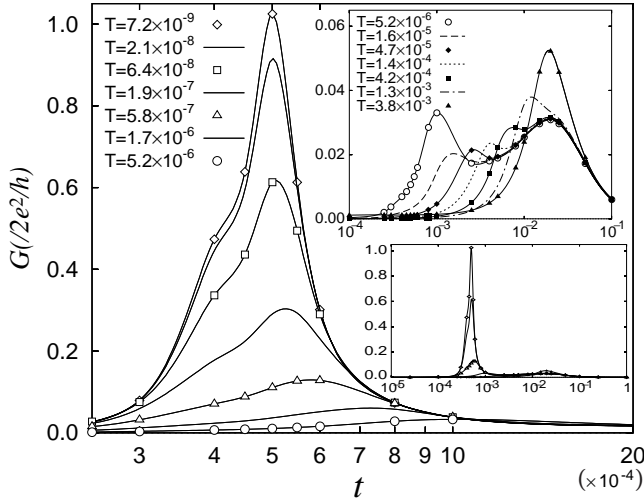


FIG. 5. Temperature dependence of the conductance. Main figure is the temperature dependence near the main peak at $t \sim 5 \times 10^{-4}$. Inset figure at the upper right is the temperature dependence near the small peak at $t \sim 2.5 \times 10^{-2}$. Inset figure at the lower right is the conductance in all over t . $\Delta/\pi U = 1.5 \times 10^{-2}$.

To discuss the characteristic behaviors of the conductance in finite temperature, we show the density of states $\rho_e(\omega)$, and the current spectrum (divided by ω) $P''(\omega)/\omega$ at $t = 5.0 \times 10^{-4}$ in Fig. 6. As the temperature increases to $T = 6.44 \times 10^{-8}$, $P''(\omega)/\omega$ at $\omega \sim 0$ become 60% of $T = 0$ limit. At the same time, $\rho_e(\omega)$ shows a small change around $\omega \sim 10^{-7}$. This means that the effect of the temperature on the conductance is rather drastic. Here we show two sorts of the magnetic excitation spectra $\chi_m''(\omega)$ and $\chi_a''(\omega)$ [9], where $\chi_m''(\omega)$ is the imaginary part of the dynamical susceptibility of the uniform magnetic moment of local spins, $(S_{L,z} + S_{R,z})/\sqrt{2}$, and $\chi_a''(\omega)$ is that of the anti-ferromagnetic moment, $(S_{L,z} - S_{R,z})/\sqrt{2}$, respectively. We show the two magnetic excitation spectra at $t = 0$ and $t = 5.0 \times 10^{-4}$ in Fig. 7. At $t = 0$, the two spectra agree with each other. However at $t = 5.0 \times 10^{-4}$, $\chi_a''(\omega)$ has the structure in

lower energy region than $\chi_m''(\omega)$. It seems that $P''(\omega)$ at the main peak of the conductance is dominated by the fluctuation given by $\chi_a''(\omega)$ from Fig. 6 and Fig. 7.

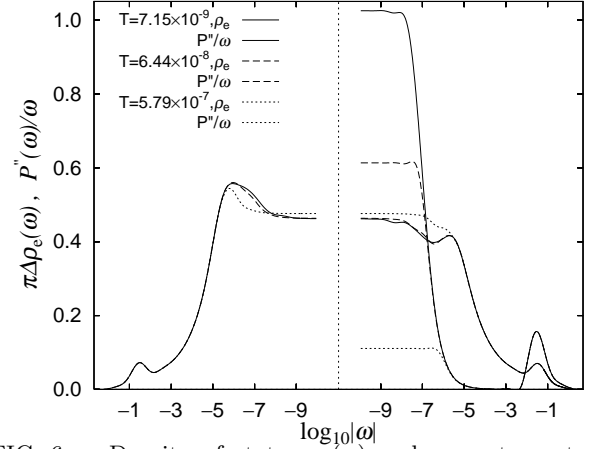


FIG. 6. Density of states $\rho_e(\omega)$ and current spectrum $P''(\omega)/\omega$ at $t = 5.0 \times 10^{-4}$ for finite temperatures. (The spectrum, which has only the positive region $\omega \geq 0$, is the current spectrum.)

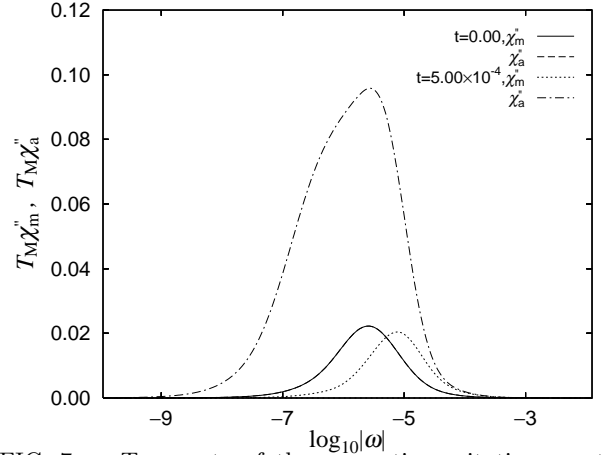


FIG. 7. Two sorts of the magnetic excitation spectra $\chi_m''(\omega)$ and $\chi_a''(\omega)$ at $T = 0$. We note that the two spectra agree with each other at $t = 0$.

We determine the two characteristic energies from $\chi_m''(\omega)$ and $\chi_a''(\omega)$ as the following ways. One is determined from the peak position of $\chi_m''(\omega)$, we call it T_M [20,28,29]. Another one, we call it T_{AF} , is determined as $T_{AF}/T_{AF,0} \equiv X_0/X$, where $X \equiv \lim_{\omega \rightarrow 0} \chi_a''(\omega)/\omega$ [9]. (And here we have $T_{AF,0} \equiv T_{M,0}$.) The suffix ‘0’ indicate ‘ $t = 0$ ’. The quantity $T_{M,0}$ almost coincides with T_K^0 . The ratio $T_{M,0}/T_K^0$ for some cases are shown in Ref. [20].

The calculated two characteristic temperatures, T_M and T_{AF} , are shown in Fig. 8. They take almost same values in $t \lesssim 10^{-4}$. T_M monotonically increases as t increasing. On the other hand T_{AF} becomes smaller near $J_{LR}^{\text{eff}} \sim T_K^0$. It has minimum of $T_{AF} \simeq 3 \times 10^{-7}$ at $t \simeq 5 \times 10^{-4}$. We note that the reduction of T_{AF}

near $T_K^0 \sim J$ had been already pointed out [8]. As t still increases, T_{AF} rapidly increases. From same analysis for the other $\Delta/\pi U$ cases, we confirm that the minimum of T_{AF} appears for the strongly correlated cases of $\Delta/\pi U \lesssim 2 \times 10^{-2}$. We show T_{AF} at the main peak position in Table. II.

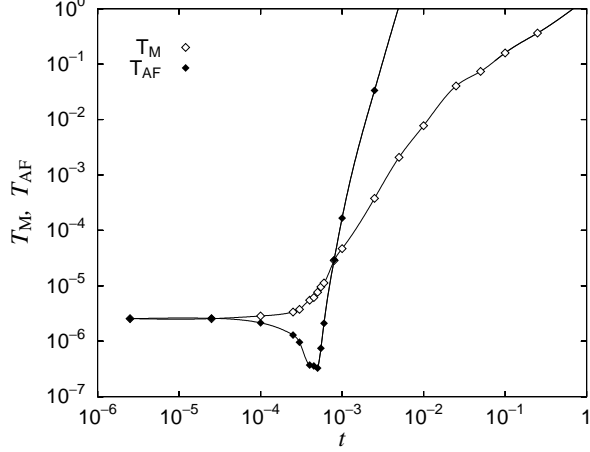


FIG. 8. Two characteristic energies T_M and T_{AF} .

From the comparison with effective parameters in Fig. 3, the larger of the effective parameters, $\max(t^{\text{eff}}, \Delta^{\text{eff}})$, and the smaller of the characteristic temperature, $\min(T_{AF}, T_M)$, almost coincide with each other in all t ,

$$\max(t^{\text{eff}}, \Delta^{\text{eff}}) \sim \min(T_{AF}, T_M).$$

Here we again see the temperature dependence of the conductance shown in Fig. 5 with the characteristic temperature shown in Fig. 8. We can see that T_{AF} characterizes the main peak of the conductance in finite temperature. The peak decreases as the temperature increases near $T \sim 1 \times 10^{-8}$ ($\sim 0.1T_{AF}(t = 5 \times 10^{-4})$) in Fig. 5. As the temperature increases and reaches to $T \sim 1 \times 10^{-6}$ ($\sim 10T_{AF}(t = 5 \times 10^{-4})$), the strength of the main peak becomes almost zero. Next we see the temperature dependence of the small peak. The small peak near $t \sim U/4 = 2.5 \times 10^{-2}$ increases as the temperature increases to about $T \sim 10^{-3}$ ($\sim 0.1T_M(t = 2.5 \times 10^{-2})$). It seems that the characteristic temperature of the conductance near the small peak is T_M . From above it seems that the characteristic temperature of the conductance is $\min(T_{AF}, T_M)$ in all t region.

Here we show the conductance from the weakly to strongly correlated cases at fixed temperatures. We show the conductance at $T = 1.6 \times 10^{-5}$ and $T = 1.4 \times 10^{-4}$ in Fig. 9. The main peak for the strongly correlated cases is sensitive to the temperature. Then the main peak of the conductance will shift to smaller t/Δ side with increasing peak height when the temperature decreases as seen from Fig. 9. This behavior will be observed as the split gate voltage is varied. We note that $T = 1.4 \times 10^{-4}$ corresponds to 16mK, and $T = 1.6 \times 10^{-5}$ corresponds to 1.9mK, for $U = 1.0\text{meV}$ systems.

$\Delta/\pi U$	1.5×10^{-2}	2×10^{-2}	3×10^{-2}	4×10^{-2}	6×10^{-2}
T_{AF}	3.28×10^{-7}	9.77×10^{-6}	3.97×10^{-4}	1.50×10^2	3.01×10^2
T_M	7.66×10^{-6}	5.64×10^{-5}	7.73×10^{-4}	3.47×10^{-3}	1.20×10^{-2}
($T_{M,0}$	2.55×10^{-6}	2.47×10^{-5}	2.31×10^{-4}	8.02×10^{-4}	3.22×10^{-3})

TABLE II. Characteristic energies at the main peak position.

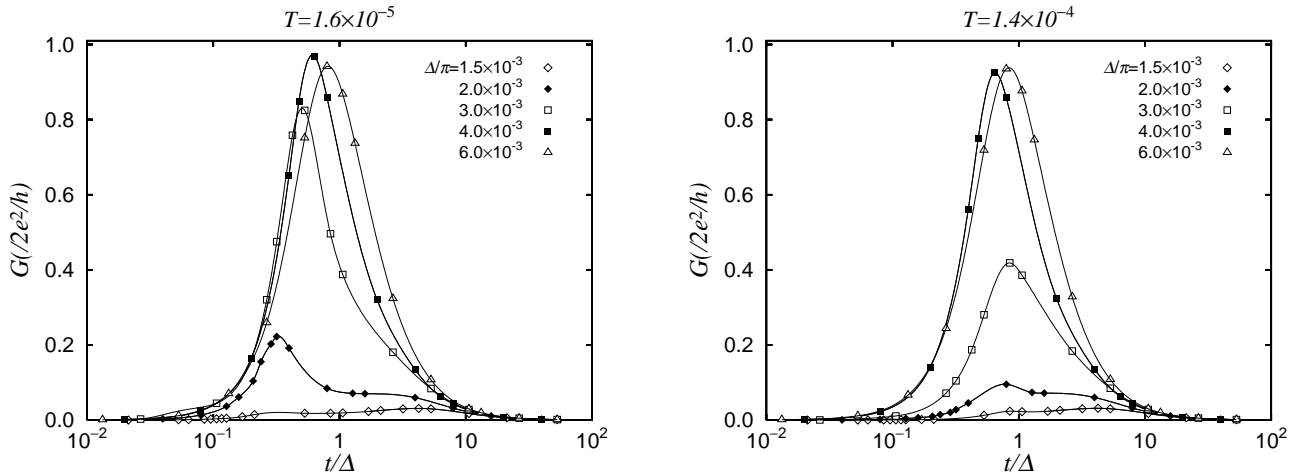


FIG. 9. Conductance from weakly to strongly correlated cases at $T = 1.6 \times 10^{-5}$ (left figure) and at $T = 1.4 \times 10^{-4}$ (right figure).

Finally, we note the accuracy of the conductance calculated from eqs. (6)-(7) by using the NRG method. It is not so accurate at very high temperatures for the small peak. In the case of $t = 0$, two dots completely decouple, then the conductance should be zero. However as shows in Fig. 10, the calculated conductance has finite value in $5 \times 10^{-3} \lesssim T \lesssim 1$ and it has maximum at $T \sim 0.05 (= U/2)$. Thus the result at very high temperatures has ambiguities. This improper finite conductance would be caused by estimation of eq. (6) at $\omega \sim T$ instead of $\omega \rightarrow 0$. The finite value in the current spectrum at $T \sim 0.05$ would reflect the largeness of the dynamical charge fluctuation in the dots.

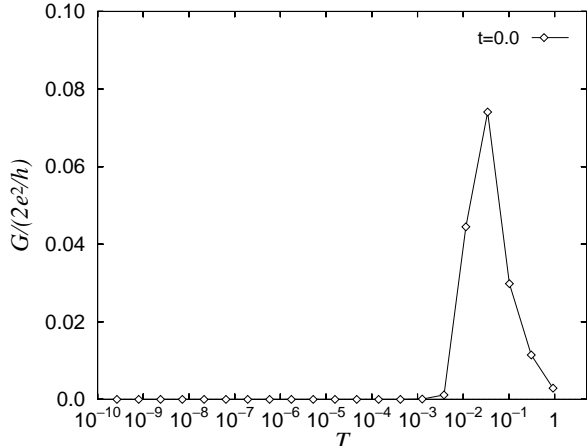


FIG. 10. Numerical results of the conductance for $t = 0$ case.

IV. SUMMARY AND DISCUSSION

We calculated the tunneling conductance through the two quantum dots that connected to the left lead and the right lead in series. We investigated the effect of the kinetic exchange coupling between the dots, and also the competition with the Kondo effect.

As the hopping between the two dots increased, (i) Kondo singlet state, (ii) local spin singlet state, and (iii) molecular orbital like state with double occupancy in even state, continuously appeared. For $t \ll U$ cases, the Kondo binding between the left (right) lead and the left (right) dot, T_K^0 , and the anti-ferromagnetic kinetic exchange coupling between the two dots, J_{LR}^{eff} , competed. The boundary between (i) and (ii) was characterized as $J_{LR}^{\text{eff}} \sim T_K^0$, and the tunneling conductance showed a peak. This peak had the unitarity limit value of $2e^2/h$ reflecting the coherent connection through the lead-dot-dot-lead. At $t \sim U/4$ of the boundary between (ii) and (iii), we had a small peak.

The system showed the strongly correlated behaviors for $\Delta/\pi U \lesssim 2 \times 10^{-2}$ ($u \equiv U/\pi\Delta \gtrsim 5$) cases. The borders of (i)-(ii) ($J_{LR}^{\text{eff}} \sim T_K^0$) and (ii)-(iii) ($t \sim U/4$) were clearly distinguished, then there were the two peak structures in the conductance. Furthermore the width of the main

peak became steeply narrow. The characteristic temperature of the main peak was strongly reduced compared with the Kondo temperature of the single dot systems T_K^0 . These anomalous behaviors of the main peak related to the quantum critical transition of the two-impurity Kondo problem studied in previously. Though the hopping term had conflicting effects on the critical transition of the two-impurity Kondo systems, generation of it through the kinetic exchange coupling and suppression of it due to the parity splitting, we found that we see the sign of the anomaly in the tunneling conductance.

The quantitative calculation shown in this paper gave the new realization for the two-impurity Kondo problem. This investigation suggested the importance of the systematic study of the DQD systems for the two-impurity Kondo problem.

ACKNOWLEDGMENTS

This work was partly supported by a Grant-in-Aids for Scientific Research on the Priority Area ‘‘Spin Controlled Semiconductor Nanostructures’’ (No. 11125201) from the Ministry of Education, Science, Sports and Culture. The numerical computation was partly performed at the Supercomputer Center of Institute for Solid State (University of Tokyo), the Computer Center of Institute for Molecular Science (Okazaki National Research Institute), and the Computer Center of Tohoku University. One of the author (W. I.) is supported by JSPS fellowship.

* izumida@eng.hokudai.ac.jp

- [1] A. C. Hewson: *The Kondo Problem to Heavy Fermions* (Cambridge University Press, 1993).
- [2] K. Yosida: *Theory of Magnetism* (Springer, 1996).
- [3] B. A. Jones, C. M. Varma and J. W. Wilkins: Phys. Rev. Lett. **58**, 843 (1987).
- [4] B. A. Jones, C. M. Varma and J. W. Wilkins: Phys. Rev. Lett. **61**, 125 (1988).
- [5] B. A. Jones and C. M. Varma: Phys. Rev. B **40**, 324 (1989).
- [6] B. A. Jones: Physica B **171**, 53 (1991).
- [7] B. A. Jones, B. G. Kotliar and A. J. Mills: Phys. Rev. B **39**, 3415 (1989).
- [8] O. Sakai, Y. Shimizu and T. Kasuya: Solid State Commun. **75**, 81 (1990).
- [9] O. Sakai and Y. Shimizu: J. Phys. Soc. Jpn. **61**, 2333 (1992); **61**, 2348 (1992).
- [10] R. M. Fye, J. E. Hirsch and D. J. Scalapino: Phys. Rev. B **35**, 4901 (1987).
- [11] R. M. Fye and J. E. Hirsch: Phys. Rev. B **40**, 4780 (1989).
- [12] R. M. Fye: Phys. Rev. Lett. **72**, 916 (1994).

- [13] I. Affleck and A. W. W. Ludwig: Phys. Rev. Lett. **68**, 1046 (1992).
- [14] I. Affleck, A. W. W. Ludwig and B. A. Jones: Phys. Rev. B **52**, 9528 (1995).
- [15] D. Goldhaber-Gordon, H. Shtrikman, D. Mahalu, D. Abusch-Magder, U. Meirav and M. A. Kastner: Nature **391**, 156 (1998).
- [16] Sara M. Cronenwett, Tjerk H. Oosterkamp and Leo P. Kouwenhoven: Science **281**, 540 (1998).
- [17] D. Goldhaber-Gordon, J. Göres, M. A. Kastner, H. Shtrikman, D. Mahalu and U. Meirav: Phys. Rev. Lett. **81**, 5225 (1998).
- [18] J. Schmid, J. Weis, K. Eberl and K. Klitzing: Physica B **256-258**, 182 (1998).
- [19] F. Simmel, R. H. Blick, J. P. Kotthaus, W. Wegscheider and M. Bichler: Phys. Rev. Lett. **83**, 804 (1999).
- [20] O. Sakai, W. Izumida and S. Suzuki: Proceedings of the 4-th Int. Symposium on Advanced Physical Field (March, 1999, Tsukuba, Japan), 143; W. Izumida and O. Sakai: Physica B (in press, Proceedings of the International Conference on Strongly Correlated Electron Systems, (August, 1999, Nagano, Japan)); W. Izumida, O. Sakai and S. Suzuki: in preparation.
- [21] For example of the recent experimental studies of the double dot systems, T. H. Oosterkamp, T. Fujisawa, W. G. van der Wiel, K. Ishibashi, R. V. Hijman, S. Tarucha and L. P. Kouwenhoven: Nature **395**, 873 (1998); T. Fujisawa, T. H. Oosterkamp, W. G. van der Wiel, B. W. Broer, R. Aguado, S. Tarucha and L. P. Kouwenhoven: Science **282**, 932 (1998).
- [22] T. Ivanov: Europhys. Lett. **40**, 183 (1997).
- [23] T. Pohjola, J. König, M. M. Salomaa, J. Schmid, H. Schoeller and Gerd. Schön: Europhys. Lett. **40**, 189 (1997).
- [24] T. Aono, M. Eto and K. Kawamura: J. Phys. Soc. Jpn. **67**, 1860 (1998).
- [25] W. Izumida, O. Sakai and Y. Shimizu: Physica B **259-261**, 215 (1999).
- [26] A. Georges and Y. Meir: Phys. Rev. Lett. **82**, 3508 (1999).
- [27] W. Izumida and O. Sakai: Physica B (in press, Proceedings of the XXII International Conference on Low Temperature Physics, (August, 1999, Espoo and Helsinki, Finland)).
- [28] W. Izumida, O. Sakai and Y. Shimizu: J. Phys. Soc. Jpn. **67**, 2444 (1998).
- [29] W. Izumida, O. Sakai and Y. Shimizu: J. Phys. Soc. Jpn. **66**, 717 (1997).